Prediction of capacitance of electrolytic capacitor with ripples

Pengchao Ye, Xiaochun Guan, Xiaojing Chen*

College of Physics and Electronic Engineering Information, Wenzhou University

Key Laboratory of Low-voltage Apparatus Intellectual Technology of Zhejiang, Wenzhou University, Chashan University Town, Wenzhou, Zhejiang Province, 325035, P.R. China

Received 1 March 2014, www.cmnt.lv

Abstract

The electrolytic capacitor is one of the most critical components in the switching power supply, in actual use of the power supply, the ripple is an important factor that leads to failure of the electrolytic capacitor. The research on the ripple's effect on the service life of the electrolytic capacitor is significant to the stability of the switching power supply. This paper designed a controllable circuit generating ripples of different phases, tested the electrolytic capacitors' changes in capacitance with ripples of different phases, analysed the reason of the changes in the capacitance, selected the fastest change, and used three prediction models of support vector regression, radial basis function and kernel-based partial least-squares algorithm to predict the change trends of capacitance of electrolytic capacitor with ripples of this phase. The results showed that compared with radial basis function and support vector regression model kernel-based partial least-squares algorithm can more accurately predict the service life of the electrolytic capacitor.

Keywords: electrolytic capacitor, ripples, different phases, prediction of capacitance, capacitor life

1 Introduction

The electrolytic capacitor is one of the most critical components in the switching power supply, and the service life of the electrolytic capacitor directly determines the service life of the power supply and other electronic devices [1]. In actual use of the power, the ripple is an important factor that leads to failure of the electrolytic capacitor [2]. Ripples of different initial phases reflect different circumstances of electrolytic capacitor failure. In the actual production process, the sampling method is often used to test quality of mass capacitors. In this paper, three prediction models of radial basis function, kernel-based partial least-squares algorithm and support vector regression can be used to test the failure time of mass capacitors to evaluate the applicability of the product. RBF network, that is, radial basis function neural network can approximate any nonlinear function, can handle the difficult regularity within the system, and has good generalization ability as well as quick learning and convergence rate, so it can be well used in the time series analysis in this experiment [3]. KPLS introduces RBF as a kernel function into partial least-squares regression, maps through the kernel function the input data into high-dimensional characteristic space, and then operates in the space, so that the nonlinear relationship between input and output variables can be established [4]. In SVR, RBF is used as the kernel function instead of the linear term in the linear equation, so that the non-linear regression can be achieved. At the same time, the kernel function is introduced to achieve the purposes of dimension rising, and increased adjustable parameters make the over-fitting still in control [5].

2 Experiment principle

2.1 EQUIVALENT FIGURE OF ELECTROLYTIC CAPACITOR

Figure 1 is the equivalent figure of electrolytic capacitor [6].

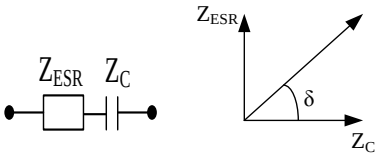

FIGURE 1 Series equivalent circuit and vector diagram

Where, Z_{ESR} is impedance of the equivalent series resistance ESR, Z_C is capacitance value of the electrolytic capacitor, and δ is the loss angle.

2.2 LOSS FACTOR OF ELECTROLYTIC CAPACITOR

Loss factor, i.e., the loss tangent, is defined as the ratio of ESR and capacitive impedance, as shown in the following Equation (1):

$$D = \tan\delta \times 100\% = \frac{ESR}{\frac{1}{\omega \times C}} = \frac{ESR}{\frac{1}{2\pi f \times C}} = 2\pi f \times ESR . \quad (1)$$

3 Experimental method and design

The experiment was carried out at room temperature. Due to room temperature for general projects, it was difficult to

* ***Corresponding author*** e-mail: chenxj@wzu.edu.cn

control the temperature. The experiment lasted one hour. The experimental subject was JAKEC electrolytic capacitor, +105°, 50V withstand voltage, 47uF. The experimental instruments used were YD2817 broadband LCR meter (to measure capacitance) and Tektronix TP2024B four-channel separated oscilloscope (to observe waveform). The frequency of ripple was 50Hz, more easily accessible, the peak value was 24V (effective value), and the ripple was not superposed on the DC component, with the effect of the DC component removed.

After each experiment, the measurement could not be done before the electrolytic capacitor was cooled to room temperature, about 2 hours. In the experiment A, five capacitors were measured for each phase, and two capacitance values were measured each time for the mean value to reduce the impact of errors. In experiment B, 20 capacitance values were measured for the mean value, and this is because as time progresses, the capacitance may vary to a small extent.

Figure 2 shows the experimental circuit. The adjusted ripple was actually the current obtained from the electric supply after transformed and half-wave rectified, whose initial phase was controlled by a single chip microcomputer. Figure 3 shows ripple voltages at different phases displayed by the oscilloscope, respectively 20°, 90° and 160°, with other circumstances omitted.

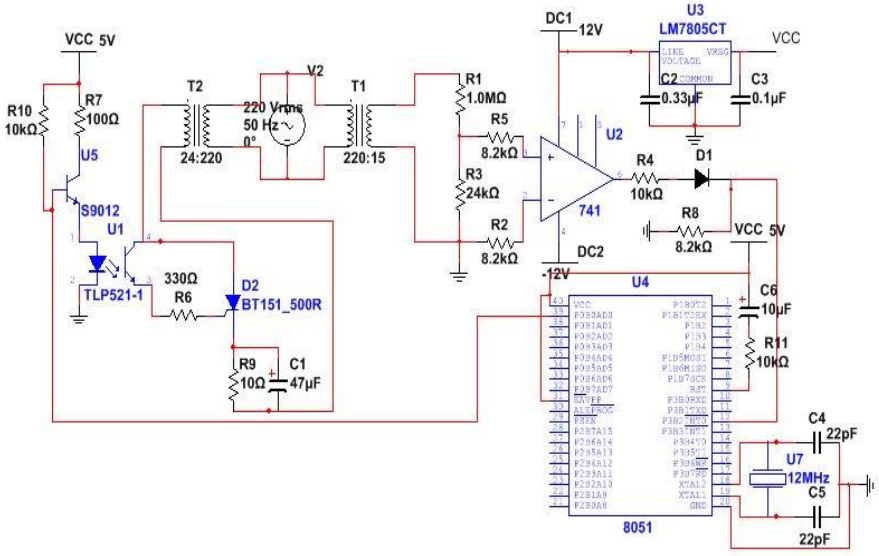

FIGURE 2 Experimental circuit diagram

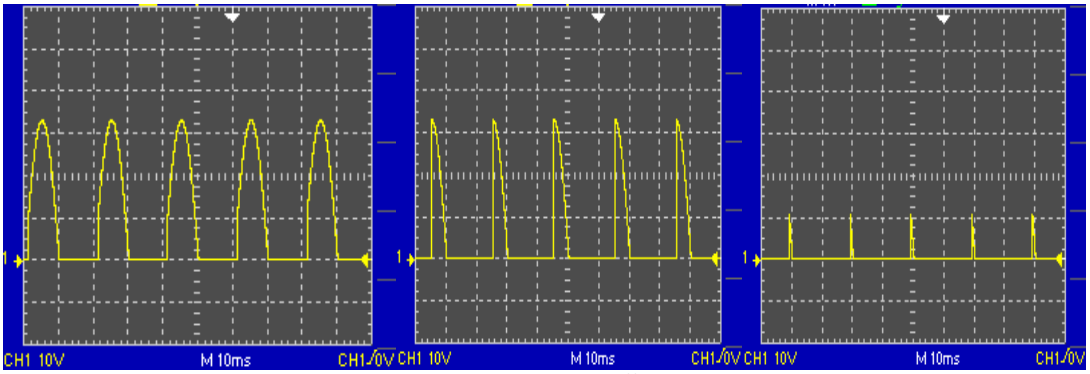

FIGURE 3 Ripple voltages at different phases

4 Results and discussion

4.1 VARIATION OF ELECTROLYTIC CAPACITOR CAPACITANCE WITH DIFFERENT PHASE RIPPLES

First, we will study the variation of electrolytic capacitor capacitance with different phase ripples, that is, loss of the electrolytic capacitor at different phases. Five capacitors were measured for each phase. The histogram (Figure 4) of the variation of electrolytic capacitor capacitance with different phase ripples can be obtained on the basis of results. Similarly, ESR of the capacitor in this case can be obtained, which is not stated here.

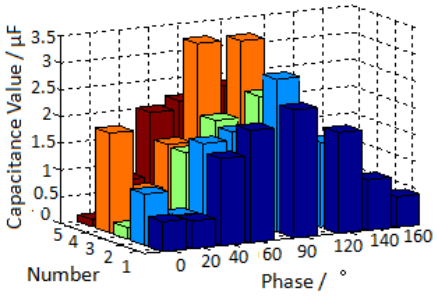

FIGURE 4 Histogram of variation of electrolytic capacitor capacitance with different phase ripples

Figure 4 shows that the ripple at 90° phase has the greatest "harm" to the electrolytic capacitor, embodied in maximum attenuation of the electrolytic capacitor of 90° in the same duration [7]. Compared to other special phases, such as 0° phase with the longest ripple duration and 160° phase with the shortest ripple duration, it is clear that at 90° phase with the highest ripple variation rate, that is, the maximum value of du/dt, rich harmonics components results in a rapid decrease of electrolytic capacitor capacitance [8, 9].

Then, we will study the ripple phase with most harms (i.e. 90° phase), and find out the variation of harm to the electrolytic capacitor with time. Figures 5 and 6 demonstrate the variation of the electrical capacitance with time.

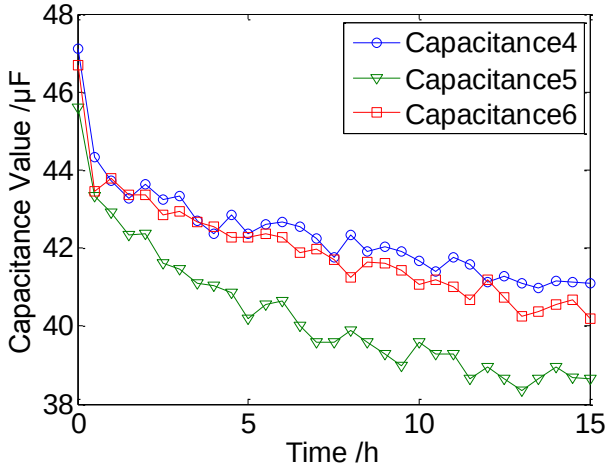

FIGURE 5 Variation of capacitance 4, 5, 6 with time (time interval of half an hour)

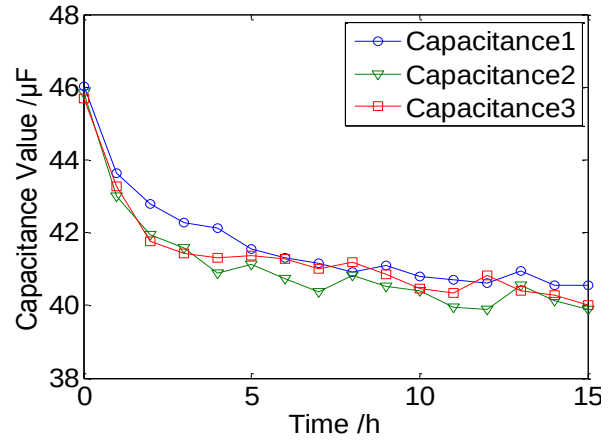

FIGURE 6 Variation of capacitance 1, 2, 3 with time (time interval of an hour)

Figures 5 and 6 show that with the ripple effect the overall trend of the electrolytic capacitor capacitance is gradual decrease, because the electrolyte repairs and thickens the oxidation film, the capacitance decreases, and ESR increases. Hydrogen generated at the cathode accelerates the volatilization of the electrolyte, resulting in degradation of the electrolytic capacitor [8]. In the early degradation, as time goes, the decrease of the capacitance becomes slow. But in the late degradation, the electrolyte has more loss and thickens, causing rise of resistivity and significantly increased loss of the capacitor [9]. But here we only study the impact of the capacitance failure in early degeneration on the circuit.

4.2 PREDICTION MODEL OF ELECTROLYTIC CAPACITOR CAPACITANCE

Figure 4 illustrates that the ripple at 90° phase has the greatest impact on the electrolytic capacitor capacitance. Figure 5 and 6 show the variation of the harm to electrolytic capacitor with time at 90° phase ripple with time, and then, we will study this trend and establish the prediction model. Capacitance 1, 2, 3 are taken as training data, Capacitance 4, 5, 6 are taken as predicted data.

First, data pre-treatment:

As in Equation (2), normalization is carried out.

$$S_{ij} = \frac{C_{ij}}{\max\limits_{j}\left(C_{ij}\right)}, \quad i = 1,2,3,4,5,6, \tag{2}$$

where, i and j are respectively the number and the moment of the capacitor sample, C_{ij} is the capacitance of the i-th capacitor at the j-th moment, $\max\limits_{j}\left(C_{ij}\right)$ is maximum value of C_{ij}, that is, the initial capacitance C_{i1} of the sample, and S_{ij} is the value of normalized C_{ij}.

As in Equation (3), equalization is carried out.

$$\bar{S}_j = \frac{\sum\limits_{i} S_{ij}}{n}, \tag{3}$$

where, n is the number of capacitor samples.

Second, as in Equation (4), by function $f(t)$ training, the data of one-hour time interval are used to train and fit the model $\bar{S}$:

$$\bar{S} = f(t), t > 0. \tag{4}$$

The training data used are $\bar{S}_j$, $j = 1, \cdots, 16$.

$\overline{s_j}$ is the value of $\bar{s}$ predicted by the fitting model at the moment j, as in Equation (5), the corresponding predicted value of the capacitor is:

$$C_{ij} = C_{i1} \times \hat{S}_j, \ i = 4,5,6, j \geq 0. \tag{5}$$

4.2.1 Neural network model

Capacitance 1, 2, and 3 are taken as modeling data, and the RBF network is applied. RBF network has two layers, the first is the implied radial basis layer, and the second is the linear output layer. Theoretically, RBF can approximate any nonlinear function.

4.2.2 KPLS model

KPLS introduces RBF as a kernel function into partial least-squares regression, maps through the kernel function the input data into high-dimensional characteristic space, and then operates in the space, so that the nonlinear relationship

before input and output variables can be established. The radial basis kernel function is selected as the kernel function.

4.2.3 SVR model

The support vector regression algorithm mainly after the dimension raising constructs in high-dimensional space a linear decision function to achieve linear regression. As e-insensitive function is used, it is mainly based on the e-insensitive function and kernel functions algorithm. If the fitting mathematical model is used to express a curve in multi-dimensional space, it, according to the results obtained by e-insensitive function, includes the curve and the "e-pipe" of the training point. In all sample points, only the sample points distributed on the "pipe wall" determine the position of the pipe. These training samples are called "support vector". To accommodate the nonlinearity of the training sample set, the traditional fitting method usually adds the higher-order term after the linear equation. Admittedly this method is effective, but the increased adjustable parameters accordingly increase risk of over-fitting. The support vector regression algorithm uses the kernel function to solve this contradiction. The kernel function is used instead of the linear term in the linear equation to make the original linear algorithm nonlinear, i.e., the nonlinear regression. At the same time, the introduction of the kernel function achieves the purpose of dimension raising, and the increase of adjustable parameters makes the over-fitting still in control. As in Equation (6), kernel functions in the above three methods are all radial basis functions and the kernel parameter is:

$$\sigma^2 = 1. \tag{6}$$

Figures 7, 8 and 9 respectively apply three prediction models of RBF, KPLS and SVR to predict the capacitance of the three capacitors of capacitor 4, 5, and 6.

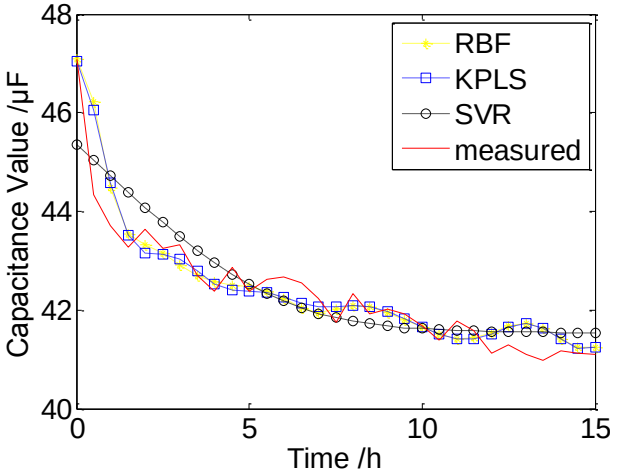

FIGURE 7 Capacitance of capacitor 4 predicted by models of RBF, KPLS and SVR

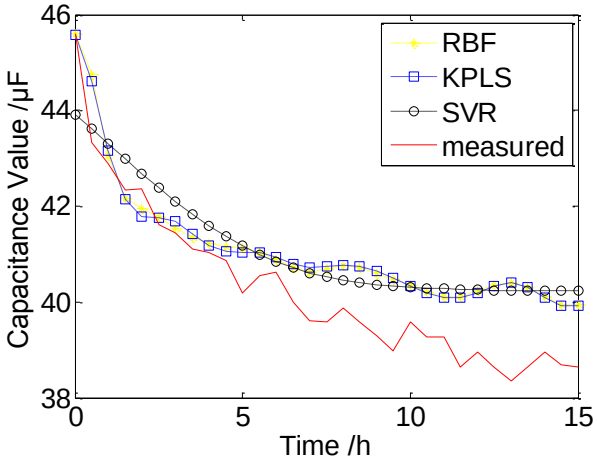

FIGURE 8 Capacitance of capacitor 5 predicted by models of RBF, KPLS and SVR

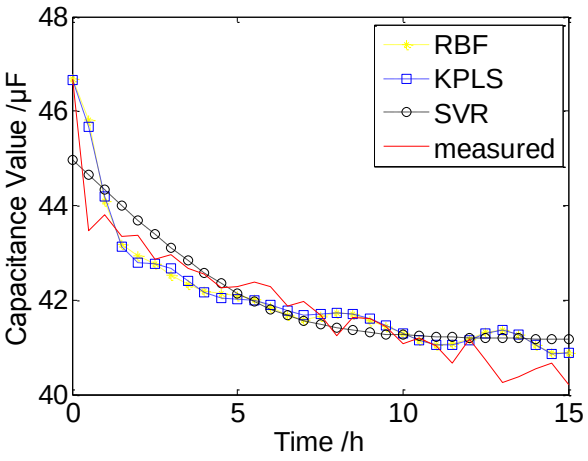

FIGURE 9 Capacitance of capacitor 6 predicted by models of RBF, KPLS and SVR

Table 1 shows mean absolute percentage error, root-mean-square error and correlation coefficient error between capacitance and measured value of the three capacitors in the three prediction models of RBF, KPLS and SVR. From Table 1, as can be seen, the root-mean-square error of KPLS is minimum.

TABLE 1 Errors of the three prediction models of RBF, KPLS and SVR

No. of capacitor	Mean absolute percentage error			Root-mean-square error			Correlation coefficient		
	RBF	KPLS	SVR	RBF	KPLS	SVR	RBF	KPLS	SVR
4	0.010	0.007	0.010	0.538	0.453	0.557	0.937	0.941	0.897
5	0.045	0.022	0.024	1.902	1.030	1.067	0.946	0.947	0.965
6	0.009	0.009	0.010	0.581	0.560	0.574	0.908	0.914	

5 Conclusion

The ripple at 90° phase has the greatest "harm" to the electrolytic capacitor, embodied in maximum attenuation of the electrolytic capacitor of 90° in the same duration. Compared to other special phases, such as 0° phase with the longest ripple duration and 160° phase with the shortest ripple duration, it is clear that at 90° phase with the highest ripple variation rate, that is, the maximum value of du/dt, rich harmonics components results in a rapid decrease of electrolytic capacitor capacitance. At the same time, we studied the curve of loss with time in case of the maximum loss. We then estimated the trend of the curve based on the above three algorithms models and found that these three models have high accuracy, KPLS is slightly better than SVR and RBF, which provides certain reference to the specific failure of the electrolytic capacitor.

Acknowledgements

The authors would like to acknowledge the financial support provided by the Program for Key Innovative Research Team of Zhejiang Province (2012R10006-0), and the Scientific Research Fund of Zhejiang rovincial Education Department (Y201223951).

Appendix A Experiment A

Table A1 Variation of electrolytic capacitor capacitance with different phase ripples

	Initial		**Final**		
Phase	*C*	*D*	*C*	*D*	*variation of C*
	46.01	0.0889	45.44	0.0961	0.56
	44.87	0.0771	43.91	0.0940	0.96
0°	45.40	0.0824	45.18	0.0863	0.22
	44.37	0.0868	42.50	0.1093	1.86
	44.35	0.0871	44.22	0.0938	0.13
	44.98	0.0751	44.46	0.0842	0.52
	45.89	0.0854	45.39	0.0907	0.51
20°	44.21	0.0849	43.86	0.0897	0.34
	45.08	0.0845	44.34	0.0898	0.73
	45.96	0.0858	45.14	0.0952	0.81
	45.63	0.0819	44.00	0.0911	1.63
	44.68	0.0860	42.89	0.0980	1.79
40°	44.78	0.0943	43.28	0.1009	1.50
	45.48	0.0830	43.94	0.0938	1.54
	45.23	0.0758	43.22	0.0960	2.02
	44.11	0.0893	42.01	0.1000	2.10
	45.40	0.0739	43.45	0.0809	1.94
60°	45.66	0.0692	43.61	0.0737	2.05
	45.33	0.0877	41.96	0.1066	3.37
	46.65	0.0731	44.48	0.0819	2.17
	46.03	0.0719	43.64	0.0747	2.39
	45.84	0.0898	42.99	0.0975	2.85
90°	45.69	0.0804	43.28	0.0825	2.41
	46.32	0.0789	42.99	0.0882	3.33
	45.28	0.0768	42.92	0.0833	2.37
	44.76	0.0934	42.88	0.0995	1.88
	46.07	0.0873	44.49	0.0951	1.59
120°	45.84	0.0882	44.49	0.0936	1.35
	45.45	0.0757	43.49	0.0882	1.96
	44.99	0.0847	43.54	0.0845	1.46
	44.99	0.0846	44.05	0.0917	0.94
	48.88	0.0624	48.05	0.0729	0.83
140°	44.98	0.0921	44.45	0.0965	0.53
	46.12	0.0890	45.47	0.0977	0.65
	45.62	0.0736	45.08	0.0786	0.53
	46.36	0.0806	45.79	0.0918	0.57
	44.99	0.1008	44.80	0.1033	0.19
160°	44.41	0.0824	44.22	0.0845	0.19
	45.68	0.0899	45.59	0.0961	0.09
	44.97	0.0757	44.77	0.0789	0.20

Appendix B Experiment B

Table B1 Variation of capacitance 1, 2, 3 with time (time interval of an hour)

	Number								
Time	*1*			*2*			*3*		
	C	*D*	*ESR*	*C*	*D*	*ESR*	*C*	*D*	*ESR*
Initial	46.03	0.0719	2.4856	45.84	0.0898	3.1197	45.69	0.0804	2.8003
1°	43.64	0.0747	2.7239	42.99	0.0975	3.6114	43.28	0.0825	3.0353
2°	42.78	0.0764	2.8438	41.96	0.1019	3.8656	41.76	0.0960	3.6606
3°	42.29	0.0742	2.7923	41.58	0.0989	3.7875	41.44	0.0929	3.5697
4°	42.12	0.0688	2.6010	40.89	0.1048	4.0817	41.30	0.0935	3.6050
5°	41.54	0.0766	2.9363	41.12	0.1015	3.9291	41.38	0.0893	3.4368
6°	41.32	0.0772	2.9751	40.73	0.1062	4.1500	41.27	0.0916	3.5328
7°	41.16	0.0804	3.1089	40.36	0.1116	4.4030	41.02	0.0965	3.7460
8°	40.92	0.0849	3.3042	40.83	0.1043	4.0677	41.20	0.0885	3.4185
9°	41.11	0.0788	3.0507	40.51	0.1088	4.2747	40.86	0.0936	3.6462
10°	40.79	0.0846	3.3026	40.42	0.1076	4.2375	40.48	0.0990	3.8948
11°	40.70	0.0856	3.3494	39.95	0.1132	4.5120	40.33	0.1009	3.9839
12°	40.60	0.0864	3.3887	39.90	0.1140	4.5482	40.83	0.0861	3.3579
13°	40.94	0.0755	2.9369	40.56	0.1034	4.0574	40.40	0.0960	3.7843
14°	40.55	0.0845	3.3186	40.14	0.1107	4.3900	40.29	0.0972	3.8401
15°	40.54	0.0843	3.3092	39.90	0.1135	4.5296	40.02	0.1023	4.0704

Table B2 Variation of capacitance 4, 5, 6 with time (time interval of half an hour)

	Number								
Time	*4*			*5*			*6*		
	C	*D*	*ESR*	*C*	*D*	*ESR*	*C*	*D*	*ESR*
Initial	47.10	0.0618	2.0893	45.61	0.0814	2.8419	46.69	0.0720	2.4556
30’	44.33	0.0849	3.0497	43.33	0.1008	3.7044	43.46	0.1038	3.8032
1°	43.71	0.0886	3.2277	42.90	0.1025	3.8046	43.80	0.0958	3.4828
1°30’	43.27	0.0904	3.3268	42.35	0.1068	4.0157	43.35	0.0968	3.5557
2°	43.64	0.0815	2.9738	42.37	0.1007	3.7845	43.37	0.0926	3.3999
2°30’	43.24	0.0843	3.1044	41.61	0.1077	4.1215	42.86	0.0979	3.6372
3°	43.32	0.0808	2.9700	41.45	0.1082	4.1566	42.95	0.0969	3.5925
3°30’	42.70	0.0892	3.3264	41.10	0.1106	4.2850	42.68	0.0982	3.6638
4°	42.37	0.0923	3.4688	41.03	0.1110	4.3079	42.55	0.0994	3.7199
4°30’	42.86	0.0842	3.1282	40.86	0.1108	4.3180	42.26	0.1009	3.8019
5°	42.38	0.0907	3.4079	40.18	0.1167	4.6249	42.28	0.1013	3.8152
5°30’	42.62	0.0849	3.1720	40.54	0.1144	4.4935	42.37	0.0959	3.6041
6°	42.67	0.0800	2.9854	40.63	0.1080	4.2327	42.28	0.0971	3.6570
6°30’	42.56	0.0799	2.9894	40.00	0.1141	4.5422	41.88	0.1022	3.8858
7°	42.24	0.0856	3.2269	39.60	0.1180	4.7449	41.96	0.1013	3.8443
7°30’	41.75	0.0923	3.5203	39.58	0.1189	4.7835	41.69	0.1044	3.9876
8°	42.34	0.0813	3.0576	39.88	0.1140	4.5519	41.24	0.1077	4.1585
8°30’	41.92	0.0878	3.3351	39.58	0.1179	4.7433	41.63	0.1047	4.0048
9°	42.03	0.0843	3.1938	39.29	0.1216	4.9282	41.61	0.1043	3.9914
9°30’	41.91	0.0852	3.2371	38.99	0.1212	4.9498	41.44	0.1053	4.0462
10°	41.68	0.0886	3.3849	39.59	0.1152	4.6335	41.08	0.1099	4.2600
10°30’	41.40	0.0928	3.5693	39.28	0.1199	4.8606	41.20	0.1100	4.2514
11°	41.77	0.0858	3.2709	39.28	0.1214	4.9214	41.02	0.1100	4.2701
11°30’	41.59	0.0878	3.3616	38.65	0.1261	5.1952	40.67	0.1143	4.4752
12°	41.12	0.0938	3.6324	38.96	0.1195	4.8842	41.18	0.1043	4.0331
12°30’	41.29	0.0907	3.4979	38.64	0.1262	5.2007	40.73	0.1132	4.4256
13°	41.11	0.0942	3.6487	38.35	0.1323	5.4933	40.26	0.1190	4.7067
13°30’	40.98	0.0956	3.7147	38.65	0.1301	5.3600	40.37	0.1183	4.6662
14°	41.17	0.0906	3.5042	38.96	0.1218	4.9782	40.54	0.1136	4.4621
14°30’	41.13	0.0901	3.4882	38.68	0.1213	4.9936	40.67	0.1108	4.3382
15°	41.10	0.0900	3.4869	38.65	0.1232	5.0758	40.20	0.1156	4.5790

References

[1] Hu X 2012 Fourier Analysis and Calculation of Electrolytic Capacitor Ripple *Skyworth Overseas Products Institute* (*in Chinese*)
[2] Xu L 2009 Modeling and Analysis of Single-phase Rectifier Capacitor Ripple Current *Nanjing University of Aeronautics and Astronautics* (*in Chinese*)
[3] Chen M 2013 MATLAB Neural Network Theory and Examples *Tsinghua University Press* 196-221 (*in Chinese*)
[4] Jia R 2013 KPLS Model based Product Quality Control for Batch Processes *School of Information Science and Engineering, Northeastern University* (*in Chinese*)
[5] Vapnik V 1995 The Nature of Statistical Learning Theory *Springer: Verlag New York Inc chapter* **6** 181-216
[6] Lin X, Hong X 2002 Aluminum Electrolytic Capacitor Engineering Technology *Xiamen University* 5-6 (*in Chinese*)
[7] Fang Y, et al 2012 Study on Ripple Rejection for Switching Power Supply *Shaanxi Province Key Laboratory of Thin Film Technology and Optical Test* (*in Chinese*)
[8] Chen Y 2003 Factors that Influence Life Test of Capacitor *Electronic Information Products Supervision Inspection Institute of Jilin Province* (*in Chinese*)
[9] Zhou H 2010 Research on Reliability of Aluminum Electrolytic Capacitor in SMPS *Harbin Institute of Technology* (*in Chinese*)

Authors

Pengchao Ye, China

Current position, grades: student of University of Wenzhou, China.
University study: Physics and Electronic Information Engineering, Wenzhou University (Communication Engineering), 2013.
Research field: information processing and testing technology.
Research direction: pattern recognition and digital signal processing.

Xiaochun Guan, China

Current position, grades: lecturer in the Wenzhou University, China.
University study: Master degree of electronic information engineering, University of Shanghai for Science and Technology in 2005.
Research activities: pattern recognition; digital signal processing; and electronic information engineering.

Xiaojing Chen, China

Current position, grades: associate professor in the Wenzhou University, China.
University study: Ph.D. degree of optical detection, Xiamen University in 2009.
Research activities: spectral analysis; pattern recognition; and digital signal processing.